

Article

An Evaluation of the Wind Energy Resources along the Spanish Continental Nearshore

Florin Onea ¹, Andrés Ruiz ² and Eugen Rusu ^{1,*} 

¹ Department of Mechanical Engineering, Faculty of Engineering, Dunarea de Jos University of Galati, 47 Domneasca Street, 800008 Galati, Romania; floryn.onea@gmail.com

² Department of Mechanical Engineering, Faculty of Industrial Engineering, Universidad de Valladolid, Paseo del Cauce, 59, 47002 Valladolid, Spain; sukoruizvelez@gmail.com

* Correspondence: eugen.rusu@ugal.ro

Received: 21 June 2020; Accepted: 21 July 2020; Published: 2 August 2020



Abstract: The main objective of the present work is to provide a comprehensive picture of the wind conditions in the Spanish continental nearshore considering a state-of-the-art wind dataset. In order to do this, the ERA5 wind data, covering the 20-year time interval from 1999 to 2018, was processed and evaluated. ERA stands for ‘ECMWF Re-Analysis’ and refers to a series of research projects at ECMWF (European Centre for Medium-Range Weather Forecasts) which produced various datasets. In addition to the analysis of the wind resources (reported for a 100 m height), the performances of several wind turbines, ranging from 3 to 9.5 MW, were evaluated. From the analysis of the spatial maps it was observed that the Northern part of this region presents significant wind resources, the mean wind speed values exceeding 9 m/s in some locations. On the other hand, in regard to the Southern sector, more energetic conditions are visible close to the Strait of Gibraltar and to the Gulf of Lion. Nevertheless, from the analysis of the data corresponding to these two Southern nearshore points it was observed that the average wind speed was lower than 8 m/s in both summer and winter months. Regarding the considered wind turbines, the capacity factor did in general not exceed 20%—however, we did observe some peaks that could reach to 30%. Finally, it can be highlighted that the Northern part of the Spanish continental nearshore is significant from the perspective of extracting offshore wind energy, especially considering the technologies based on floating platforms. Furthermore, because of the clear synergy between wind and wave energy, which are characteristic to this coastal environment, an important conclusion of the present work is that the implementation of joint wind–wave projects might be effective in the Northwestern side of the Iberian nearshore.

Keywords: wind power; turbines; offshore; Iberian Peninsula; efficiency; ERA5

1. Introduction

Climate change is an issue that must be confronted imminently. On the other hand, the continuous growth of the global population brings with it an increase in energy demand that exacerbates the emissions of polluting gases, a problem produced by the fossil fuel-based energy industry [1]. Renewable energies are those whose natural source is virtually inexhaustible and that also do not generate emissions of polluting gases such as CO₂ into the atmosphere. From this perspective, the progress in the measures taken against climate change brings with it an inherent growth of this energy sector. Furthermore, it is considered that supporting renewable energy brings benefits beyond the ecological, such as the reduction of the national energy dependence and it is directly related to the country’s GDP (gross domestic product) growth. Thus, it is not surprising that the European Union and several governments around the world keep showing growing support to the renewable industry [2,3]. The society is also gradually moving towards more sustainable production methods

and trying to reduce waste generation and gas emissions on a personal level, so this social support for renewable energies represents another driver of this change [4,5].

One of the renewable energies, which utilization has proven to be more viable, is wind energy. This is the cheapest renewable energy source and is already a well-established sector that has seen stable growth for decades. Traditionally, wind farms have been located onshore and great technological development has been achieved for this type of installation, the actual trend being to increase the dimensions of the turbines in order to generate more energy [6]. In recent years, the creation of offshore wind farm projects has also gained increasing importance [7]. The remarkable energetic characteristics of the wind in these coastal areas, where there are normally fewer irregularities and the wind speed is usually higher than onshore, has awakened a general interest for the offshore wind energy [8,9]. Fixed offshore wind turbines can operate until about 60 m depth and base their technology on the already well-developed onshore turbines, the type of foundation that is used being the main difference. On the other hand, the floating turbines allow the location of these farms in areas farther away from the coast, where the depth of the seabed is greater [10,11].

The present study focuses on Spain, more specifically on the Spanish coastal environment along the Iberian Peninsula. Spain is a country with notable characteristics for the usage of its renewable sources, with a Mediterranean climate that makes its solar and wind energy of special interest. Furthermore, taking into account the scarcity of the fossil resources of the territory, it is feasible to consider renewable energies as the main energetic potential of the country [12,13]. With more hours of sun per day than almost any other country in the European Union, and with little variability of the solar characteristics throughout the country, the usage of solar energy for both electricity and thermal energy production is something that has a well-developed character in the country. However, wind energy shows the highest growth at the moment. This translates into a rapid increase in the nominal installed capacity of the wind energy in the country, which has experienced huge growth during the last decades. The implementation of new wind energy projects is being promoted and financially supported by the Spanish government, which tries to overcome the administrative barrier caused by the lack of an already well established legal framework for this industry [14].

These administrative barriers are even greater when related to the offshore wind energy. This among others is one of the reasons that lead to the nonexistence of working offshore wind farm installations actually located in Spain, despite the great length of the country's coastal environment. The great depth of the seafloor represents one of the main bathymetric characteristics of the Spanish coast, while the existence of the environmental exclusion zones along the nearshore is another important reason for the lack of working offshore wind farms. Moreover, there exists a clear need to develop the aforementioned floating turbine technology, so that these can be located in deeper waters [15]. However, although the lack of operating facilities at the moment is not the main focus of the Spanish offshore wind industry, the government—supported by the European Union—continues to work in order to facilitate the implementation and development of this type of projects. The rapid development of the floating technologies is expected to take out the seafloor depth as well as the environmental exclusion zone related issues in what can be considered the near future [16,17]. In Colmenar-Santos et al. [15], these and further characteristics related to the future of the offshore wind industry in Spain are discussed, concluding that once the techno-economic and administrative barriers are surpassed, Spain counts with good prospects for the further development of the offshore wind installations.

Currently, there is a large project for the installation of a floating offshore wind farm in the Spanish territory of the Canary Islands. Endorsed by the Norwegian company Equinor, it will entail an investment of more than 860 million euros and with a nominal installed capacity of 200 MW, it is expected to be completed during the year 2024 [18,19]. As a first step, this project will establish the country's offshore wind standard, and when completed will lead to the creation of new offshore wind projects. On the other hand, the Northern part of the Iberian nearshore also has considerable wave energy [20,21] and from this perspective this area is among the most representative coastal environments in regards to the combined wind-waves energy resources [22] where hybrid projects

can be successfully implemented. In this context, the present work seeks to evaluate the energetic characteristics of the wind in the Iberian nearshore along the Spanish coastal environment. The outcome of the work is to provide a global image that allows to identify areas of interest where the wind energy resources are more significant, and to establish the behavior that a selected number of turbines would have if located in the mentioned hot-spots in order to determine the viability of an offshore wind farm installation.

2. Materials and Methods

2.1. The Target Area

The Spanish shore has a length of 7905 km, where 5978 km are located along the Iberian Peninsula. In the present study, the Spanish peninsular coast was divided in two separate sectors. As shown in Figure 1, the North sector corresponds to the Atlantic coast located in the Northern part, and the South sector, corresponding to the Mediterranean coast is located along the Southern and Eastern parts of the Spanish territory. For the present study, 20 points along the Spanish nearshore were considered, 10 of them being located in the North sector and the remaining 10 along the South sector. Given that one of the main bathymetric characteristics of the Spanish coastal environment is the rapid descent of the continental shelf, the possibility of selecting the study points based on the depth of the seafloor was quickly discarded, and therefore the following selection method for the offshore points considered for analysis was developed.

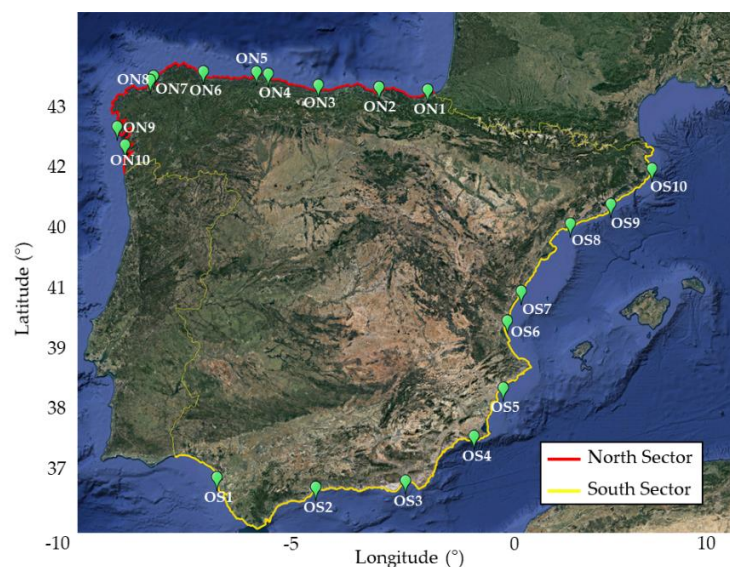


Figure 1. The Iberian Peninsula and the locations considered (map processed from Google Earth, 2020).

Spain counts with a national public entity denominated Puertos del Estado with responsibilities regarding the Spanish Port System [20]. Given that Spain is one of the European countries with more kilometers of coast, it is meaningful to highlight the importance of the mentioned institution on a national and international level. Among other functions, the one of interest for the present study is compiling and analyzing coastal wind information such as wind speed. With this objective, there are a series of meteorological stations on locations of geographical relevance along the entire Spanish coastal environment [21]. Considering this, for the selection of the 20 study points located on the sea, and foreseeing the fact that in subsequent studies a comparative of the offshore and onshore wind capacity and energetic characteristics might be of interest, an initial selection of 20 of these stations located on land was made. After that, we decided to locate the offshore points at a distance of five kilometers into the sea, measured perpendicularly to the coastline, from each of the 20 land points

mentioned previously. These offshore study points, represented on Figure 1, were denominated ON1 to ON10 for those located on the Atlantic coast, ON indicating Offshore North.

Subsequently, the points located in along the Spanish Mediterranean coast were denominated OS1 to OS10, OS indicating Offshore South. These selected study points are distributed along the entire Spanish nearshore and geographically related one to one to the 20 main meteorological stations of Puertos del Estado. Table 1 presents the main characteristics of the 20 offshore locations considered for the study [22].

Table 1. The main characteristics of the offshore locations considered.

| Sector | Point | Long (°) | Lat (°) | Water Depth (m) | Distance from Coastline (km) |
|--------|-------|----------|---------|-----------------|------------------------------|
| N | ON1 | -1.94 | 43.38 | 88.22 | 5 |
| N | ON2 | -3.08 | 43.42 | 63.33 | 5 |
| N | ON3 | -4.5 | 43.44 | 102.5 | 5 |
| N | ON4 | -5.68 | 43.61 | 43.15 | 5 |
| N | ON5 | -5.96 | 43.64 | 49.8 | 5 |
| N | ON6 | -7.21 | 43.61 | 74.95 | 5 |
| N | ON7 | -8.38 | 43.49 | 50.2 | 5 |
| N | ON8 | -8.45 | 43.42 | 64.75 | 5 |
| N | ON9 | -9.14 | 42.59 | 52.25 | 5 |
| N | ON10 | -8.92 | 42.29 | 64 | 5 |
| S | OS1 | -6.48 | 36.78 | 11.6 | 5 |
| S | OS2 | -4.38 | 36.67 | 61 | 5 |
| S | OS3 | -2.48 | 36.79 | 77.31 | 5 |
| S | OS4 | -1.01 | 37.53 | 87.1 | 5 |
| S | OS5 | -0.36 | 38.33 | 58.4 | 5 |
| S | OS6 | -0.24 | 39.46 | 38.2 | 5 |
| S | OS7 | 0.09 | 39.95 | 29.65 | 5 |
| S | OS8 | 1.27 | 41.06 | 62.65 | 5 |
| S | OS9 | 2.24 | 41.36 | 60.45 | 5 |
| S | OS10 | 3.28 | 41.93 | 169.6 | 5 |

2.2. Wind Dataset

For the reanalysis made in the present study, the historical database ERA5 [23], successor to the well-established ERA-Interim was considered [24]. This database is the latest global atmospheric reanalysis created by the European Centre for Medium-Range Weather Forecast (ECMWF), covering the time period from 1950 to five days behind real time.

This time series of historical data compiles information on atmospheric parameters at land and sea level with a time resolution of 1 h and a high spatial resolution of $0.25^\circ \times 0.25^\circ$ (about 31 km²). The model provides hourly wind and atmospheric pressure fields consistent with the previous evolution of the modeled parameters [25].

The study considers the time series of historical values for wind speed at 10 m height during the 20-year period from 1999 to 2018 on the selected offshore study points along the Spanish offshore environment, with a time resolution of 6 h (associated with 00:00-06:00-12:00-18:00 UTC). With these data, a statistical analysis using the computing tool MATLAB was made in order to identify some relevant wind parameters of interest at the selected locations [26].

2.3. The Wind Technologies Considered

For the present study, it is of great relevance to evaluate not only the energetic characteristics of the wind along the Spanish coastal environment, but also to study how different wind turbine technologies would perform. Thus, by studying operational parameters that certain wind turbines would have if located in the considered locations, the conclusions of the study will improve their validity in identifying hot-spots along the Spanish nearshore, as well as determining the feasibility of developing an offshore wind farm installation.

From this perspective, the authors selected four different wind turbine technologies with a wide range of operational characteristics in order to obtain a better representation of the working performance that an offshore wind farm would obtain. The wind technologies considered for evaluation in the present work are outlined in Table 2, since the present study seeks to analyze the present viability of an offshore wind project, all of the selected technologies are currently installed and operating in other wind farms. Thanks to this, the results of the present study do not rely on any future technological developments [27–30].

Table 2. Technical specifications of the technologies considered.

| Turbine | Rated Power (MW) | Cut-In Speed (m/s) | Rated Speed (m/s) | Cut-Out Speed (m/s) | Hub Height (m) | Reference |
|-------------|------------------|--------------------|-------------------|---------------------|----------------|-----------|
| V90-3.0 MW | 3 | 4 | 15 | 25 | 80–105 | [30] |
| M5000-116 | 5 | 4 | 12.5 | 25 | 90 | [27] |
| V164-8.8 MW | 8.8 | 4 | 13 | 25 | 105–140 | [28] |
| V164-9.5 MW | 9.5 | 3.5 | 14 | 25 | 105–140 | [29] |

In order to study a wide range of rated capacities, this parameter varies from 3 to 9.5 MW, while the corresponding power curves associated to the wind turbines are presented in Figure 2. It is worth noting the differences on how the power curve of each wind turbine evolves when increasing the velocity until each one reaches its characteristic cut-in speed. The differences on this value, beyond being somewhat arbitrary, is another of the characteristics that determines the different operational energetic parameters that each turbine would obtain when installed. Although each turbine is defined by different hub heights, all the systems will be evaluated for a hub height of 100 m above the sea level for the present work. Thus, the selected technologies present a wide range of operational characteristics, and it can indeed lead to different turbines performing better or worse than others depending on the studied location [8,31,32].

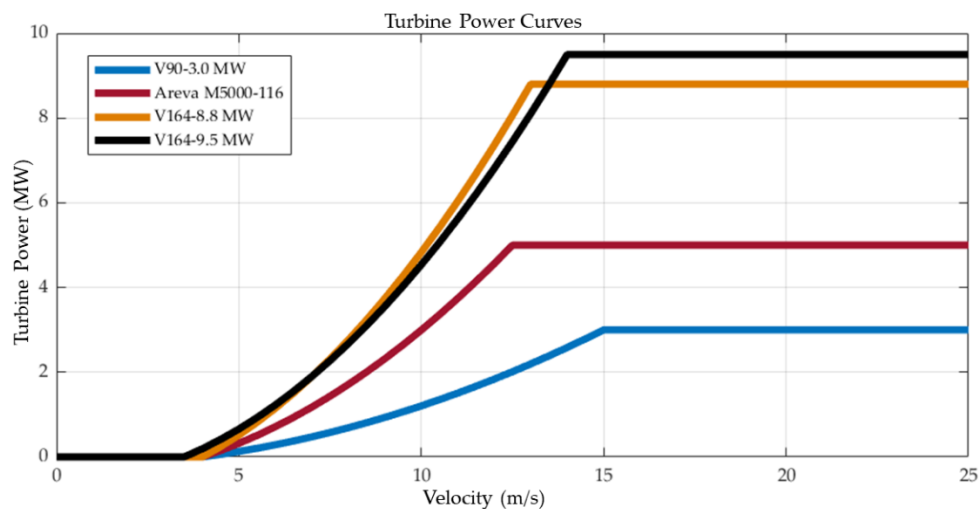


Figure 2. Power curves of the selected wind turbines.

2.4. Methods

In order to study the aforementioned dataset, a series of relevant characteristic wind parameters were obtained, as well as some operational parameters considered relevant for the wind turbines. The wind speed values provided by the dataset ERA5 are reported at a height of 10 m above sea level, however, in order to study this parameter at 100 m, which is the considered operational height of the turbines in this study, it is necessary to apply a logarithmic law that has the following form [33]:

$$U_z = U_{z\text{ref}} \frac{\ln\left(\frac{z}{z_0}\right)}{\ln\left(\frac{z_{\text{ref}}}{z_0}\right)}, \quad (1)$$

where U_z represents the wind speed at a certain height z , here mentioned as the operational height of the turbines, 100 m above sea level. The parameter $U_{z_{ref}}$ represents the known value of the wind speed at a given height z_{ref} , in this case being 10 m above the sea level, and finally z_0 represents the roughness length, which in this study is estimated to have a value of 0.0002 m [31]. By applying the logarithmic law, the study is able to consider the wind speed values at a reasonable operational height for the different wind turbine technologies considered, and in this way to study the different operational statistical parameters of interest.

At this point it is important to mention that among the ERA5 product, a wind dataset reported at 100 m height is available, so it will be important to notice the differences between the adjusted U_{100} values and this product. By extrapolating the wind speed from 10 to a 100 m height, it is possible to add a higher uncertainty that may influence the statistical results. In Table 3, such an evaluation is presented by considering all the points and the values reported for the full-time distribution. The differences (in m/s) between the two datasets are indicated in percentiles. In general, the North points reveal a better agreement, also noticing an increase of the variations as we go from 25th to 95th. Positive values are reported only by the 25th, expecting minimum values (< 0.1 m/s) for the points ON1, ON4, ON5, ON10, OS7, OS9, and OS10, respectively.

Table 3. Percentile values—direct comparison reported between the U_{100} parameters (logarithmic law) and the U_{100} parameters provided by the ERA 5 project. The results (in m/s) are reported for the 20-year time period of wind data (1999–2018) where: the positive values indicate that the adjusted U_{100} values are much higher; negative values indicate a reverse trend.

| Percentiles | ON1 | ON2 | ON3 | ON4 | ON5 | ON6 | ON7 | ON8 | ON9 | ON10 |
|-------------|-------|-------|-------|-------|-------|-------|-------|-------|-------|-------|
| 25th | 0.06 | −0.03 | 0.14 | 0.01 | 0.05 | −0.3 | −0.42 | −0.46 | −0.11 | 0.02 |
| 50th | −0.12 | −0.16 | 0.09 | −0.17 | −0.12 | −0.66 | −0.72 | −0.79 | −0.47 | −0.4 |
| 75th | −0.59 | −0.65 | −0.07 | −0.43 | −0.33 | −0.96 | −1.02 | −1.06 | −0.78 | −0.76 |
| 95th | −1.24 | −1.21 | −0.39 | −0.74 | −0.61 | −1.76 | −1.67 | −1.68 | −1.22 | −1.18 |
| Percentiles | OS1 | OS2 | OS3 | OS4 | OS5 | OS6 | OS7 | OS8 | OS9 | OS10 |
| 25th | −0.46 | −0.03 | −0.11 | 0.15 | −0.05 | −0.16 | 0.01 | −0.21 | 0.05 | 0.09 |
| 50th | −0.74 | −0.21 | −0.29 | 0.01 | −0.11 | −0.38 | −0.13 | −0.33 | −0.07 | −0.11 |
| 75th | −1.01 | −0.52 | −0.59 | −0.16 | −0.37 | −0.74 | −0.35 | −0.58 | −0.22 | −0.29 |
| 95th | −1.33 | −0.9 | −0.88 | −0.44 | −0.81 | −1.66 | −1.37 | −1.55 | −0.93 | −0.31 |

Regarding the North points, the differences significantly increase from ON1 to ON10, reaching a maximum of 0.46, 0.79, and -1.06 m/s for ON8 (25th, 50th, and 75th) while a 1.76 m/s is accounted by ON6 (95th). As for the South points, the differences are distributed in the range of 0.01 and 0.46 m/s (OS7-OS1/25th); 0.01 and 0.74 m/s (OS4 and OS1/50th); 0.16 and 1.01 m/s (OS4 and OS1/75th); and 0.31 and 1.66 m/s (OS10 and OS6/95th). In order to avoid any confusion, in the present work we will use the wind dataset that consider the U_{10} wind conditions adjusted throughout the logarithmic law.

Having applied the logarithmic law and consequently obtained the wind speed values at the considered wind turbine operational height, the wind characteristics of interest can be studied. The parameter wind power density (P_{wind} in W/m^2) allows one to determine the energetic potential of the wind in a specific location, and it is defined as [31,34]:

$$P_{wind} = \frac{1}{2} \rho_{air} (U_z)^3, \tag{2}$$

where U_z again represents the wind speed at a certain height z above the sea level (100 m in this case), and ρ_{air} is the air density at said height, which in this study is estimated to be 1.225 kg/m^3 [31].

Once these parameters have been obtained, subsequent classifications can be made regarding the wind energetic capacity on each location. With this objective, it is widely common to classify wind capacities by classes, going from C1 to C7 [35,36]. These classes are based on the wind speed magnitude and going from lower to higher wind speed they consequently provide information on the

attractiveness of each of the locations with a view to the location of an offshore wind farm, being those with higher class winds more interesting for this possible development [35].

Just as wind capacity is classified based on the magnitude of its speed, turbine technologies are classified based on their operational wind speed characteristics [32]. Considering that each turbine entails a large economic investment, it is of great importance ensuring that, when determining the viability of an offshore wind farm project, the wind turbine technologies considered will operate efficiently and without suffering any type of catastrophic failure during their operational life span under the conditions to which they will be subjected. In order to ensure this, a subsequent classification for wind turbines can be applied, created by the International Electrotechnical Commission (IEC), it is a safety standard followed by the European Union that classifies the turbines according to the wind speed at which they have been designed to work [32,37,38]. In the technical specification of a wind turbine, for each system mentioned there is an IEC wind class, which indicates that a wind turbine will efficiently operate for a particular wind condition. A turbine class is defined by several parameters, such as the average wind speed, turbulence intensity, or 50-year wind gust. In the present work, only the average wind speed was taken into account, covering all the four wind classes, namely: C1—10 m/s, C2—8.5 m/s, C3—7.5 m/s, and C4—6 m/s.

Due to the fact that irregularity is one of the main characteristics of the wind, it is also interesting to evaluate how the magnitude of the wind speed (U_{100}) fluctuates considering different periods of time [8,39]. This irregularity can lead to locations where the wind has notable wind energetic characteristics during determined months or seasons, having a lower annual mean than other points that have lower but steadier and consistent values all year around. To evaluate this, the monthly means for the wind speed values at operative height are studied as well as the seasonal variability on each of the locations considered. The seasonal variability was obtained with the following equation [8]:

$$Seasonal = \frac{P_{S_{windmax}} - P_{S_{windmin}}}{P_{S_{windaverage}}}, \quad (3)$$

where $P_{S_{windmax}}$ and $P_{S_{windmin}}$ represent the maximum and minimum wind power capacity (P_{wind}) values for all the seasons and $P_{S_{windaverage}}$ represents the average value for the 20-year period.

In order to apply statistical methods to the wind speed parameter, it is necessary to use a probability distribution that defines it. In general, the two-parameter Weibull distribution, being the most used distribution in the study of the offshore wind farms, and given that the wind speed accurately adapts to it, is widely considered to precisely define this parameter [40]. The probability of the wind speed, U , of the Weibull distribution follows the formula [41]:

$$f(U) = \frac{k}{c} \left(\frac{k}{v}\right)^{k-1} \exp\left[-\left(\frac{v}{c}\right)^k\right], \quad (4)$$

where k and c are the characteristic parameters of the Weibull distribution approached by the wind speed parameter at each of the locations considered, with the mention that c parameter is measured in m/s and always have a value equal or higher to zero [39]. The parameter k is defined as the shape parameter and is an indication of the variability of the wind speed values, depending on the width or narrowness of the distribution curve. The parameter c is the scale parameter of the distribution and indicates the magnitude of the wind speed values. The use of this distribution provides the possibility of modifying the value of the aforementioned dimensionless parameters in order to ensure that the distribution adapt correctly to different time periods. In this way, it is possible to obtain monthly or seasonal Weibull distributions that precisely define the wind speed [8,42].

Once the Weibull probabilistic distributions have been defined for each of the locations considered for a determined period of time, statistical methods can be applied to the wind speed parameter. In this way, the authors proceed to study parameters that provide insight to the performance for the selected wind speed turbine technologies. In the study, each of the four selected wind turbines are defined by a

different characteristic power curve [31]. By studying them on each of the locations considered, it is possible to obtain the energetic parameter known as Annual Electricity Production (AEP in MWh). Its value determines the amount of electric energy produced by a certain wind turbine in a given location during an established period of time. There are different approaches that can be considered in order to calculate this parameter, and in the present study the following formula is used [31,43]:

$$AEP = T \times \int_{cut-in}^{cut-out} [f(U)P(U)] dU. \quad (5)$$

The parameter T represents the number of hours that the wind turbine will operate during a year, which in this study is considered to be equivalent to 8760 h/year [8]. The parameter $f(U)$ is the Weibull probability function followed by the wind speed at the turbine location, $P(U)$ is the characteristic power curve of the turbine and the integration limits cut-in to cut-out correspond respectively to the minimum and maximum value of the wind speed at which the turbine is working. With wind speeds below the cut-in value, the turbine does not produce electrical power, and with higher wind speeds it operates normally until it reaches the wind turbine characteristic rated power [44,45]. Above this level of energy production, which occurs at a given wind speed, the possibility of the wind turbine suffering a catastrophic failure gains weight and in order to avoid this, a braking system known as cut-out is activated.

Another parameter that provides information of the wind turbine performance is the capacity factor (C_f) [8], which is a dimensionless ratio that relates the energy output of a turbine during a determined period of time, with the ideal maximum possible output that could have been obtained in that period. This maximum possible output considers that the wind turbine would operate continuously at full nameplate capacity during the studied period of time. Given that this is not a realistic occurrence, the value of the ratio is always under 100%. In the study it is obtained using the formula [8,46]:

$$C_f = \frac{P_{turbine}}{P_{rated}} \times 100, \quad (6)$$

where $P_{turbine}$ (in MW) is the theoretical energy output of the wind turbine and P_{rated} (in MW) represents the rated power of the studied turbine.

Lastly, and coming back to the main nature of renewable wind energy, which after all is the possibility of reducing the contaminant gas emissions to the atmosphere in order to reduce the future impacts of climate change and the subsequent global warming, it is of special interest to study the parameter known as CO₂ equivalent emission avoidance [47]. This parameter allows both to estimate the amount of CO₂ that would cease to be emitted if the project is carried out, as well as the amount of CO₂ that is currently ceased to be emitted by an already established project that has been operating for a determined time period. In this study the value is obtained using the formula [48]:

$$CO_{2emissions} = AEP \times x \times y, \quad (7)$$

where $CO_{2emissions}$ is the avoided emission rate (in tons CO₂/MWh), AEP represents the aforementioned parameter denominated as annual electricity production of the wind turbine considered, x is the reductions of kilowatt-hours into avoided units of carbon dioxide emissions with a value of $x = 6.62 \times 10^{-4}$, and y converts metric tons to tons $y = 1.102311$.

3. Results

This section presents the results obtained by studying the aforementioned parameters for each of the locations considered. Thus, Table 4 represents the seasonal and total means for the 20-year period considered in each of the North sector points. Similarly, Table 5 shows the same information for the remaining 10 points located in the South sector. It is obvious to observe that in the North Sector, the points that show the highest averages are located on the most Western part of the Iberian Peninsula.

Thus, the reference point ON7 with a maximum winter mean of 7.5 m/s, is the location that presents the highest mean for three out of the four seasons. This is only slightly surpassed by ON9, with a summer mean of 6.17 m/s. The point ON7 shows the highest total mean with a magnitude of 6.75 m/s for the time period considered.

Table 4. Mean wind speed values (U_{100}) by season and total for the points located in the North sector.

| Point | Winter (m/s) | Spring (m/s) | Summer (m/s) | Autumn (m/s) | Total (m/s) |
|-------|--------------|--------------|--------------|--------------|-------------|
| ON1 | 5.72 | 4.85 | 3.99 | 4.81 | 4.84 |
| ON2 | 5.81 | 4.95 | 4.07 | 4.9 | 4.93 |
| ON3 | 4.61 | 4.28 | 3.87 | 4.09 | 4.21 |
| ON4 | 5.58 | 5.08 | 4.41 | 4.91 | 4.99 |
| ON5 | 5.98 | 5.38 | 4.6 | 5.19 | 5.29 |
| ON6 | 6.09 | 5.42 | 4.64 | 5.22 | 5.34 |
| ON7 | 7.5 | 6.9 | 6.03 | 6.57 | 6.75 |
| ON8 | 7.26 | 6.68 | 5.8 | 6.33 | 6.51 |
| ON9 | 7.19 | 6.85 | 6.17 | 6.33 | 6.63 |
| ON10 | 6.5 | 6.19 | 5.54 | 5.64 | 5.97 |

Table 5. Mean wind speed values (U_{100}) by season and total for the points located in the South sector.

| Point | Winter (m/s) | Spring (m/s) | Summer (m/s) | Autumn (m/s) | Total (m/s) |
|-------|--------------|--------------|--------------|--------------|-------------|
| OS1 | 5.25 | 5.49 | 4.72 | 4.69 | 5.04 |
| OS2 | 4.44 | 4.02 | 3 | 3.49 | 3.74 |
| OS3 | 4.85 | 5.29 | 4.33 | 4.62 | 4.77 |
| OS4 | 5.99 | 5.89 | 5.18 | 5.5 | 5.64 |
| OS5 | 4.6 | 4.5 | 3.96 | 4.2 | 4.31 |
| OS6 | 4.28 | 3.98 | 3.44 | 3.66 | 3.84 |
| OS7 | 3.82 | 3.79 | 3.3 | 3.51 | 3.61 |
| OS8 | 4.8 | 4.38 | 3.65 | 4.05 | 4.22 |
| OS9 | 4.18 | 4.1 | 3.54 | 3.92 | 3.93 |
| OS10 | 7.26 | 6.53 | 5.9 | 6.77 | 6.61 |

Despite the fact that the locations of the South sector generally present lower values, two of the points have similar values to the ones from the North sector. Point OS4 presents similar means to the ones from the Atlantic Coast. This is to be expected since the geographical characteristics of the Strait of Gibraltar, where it is located, cause that with the existence of wind coming from the Mediterranean Sea, creating a Venturi effect, which is characterized by a drop in the atmospheric pressure that comes with an increase of the Westerly wind speed values. However, the location along the Mediterranean Coast with the highest means is the point OS10, with a maximum winter average wind speed of 7.26 m/s and a total average of 6.61 m/s.

The total mean values for the full time period considered shown in the previous tables are complemented by Figure 3, a map of the spatial distribution of the wind resources (U_{100}) along the entire Spanish coastal environment. This is a clear graphic representation of all the aspects mentioned above. For its part, the changes in the values of the seasonal means than can be observed in the Table 3, are graphically represented in the Figure 4, where the seasonal variability of the wind speed (U_{100}) along the Spanish nearshore is mapped.

Figure 5 illustrates the distribution of the U_{100} mean considering a time span of one month for the points of the North sector, while Figure 6 provides the same representation for the South sector points. It is noticeable that, as expected, these figures show values consistent with those already presented in Figure 4, with general higher values in the months of November to February, and general decrease in the summer months. In the North sector, the values are between a maximum mean of 7.57 m/s for the ON7 location during July, and 3.74 m/s, minimum mean that represents the month of September in the ON10 location. The values of the South sector go from 2.85 m/s during August in the point OS2 to the highest value of 7.67 m/s in OS10 location during November.

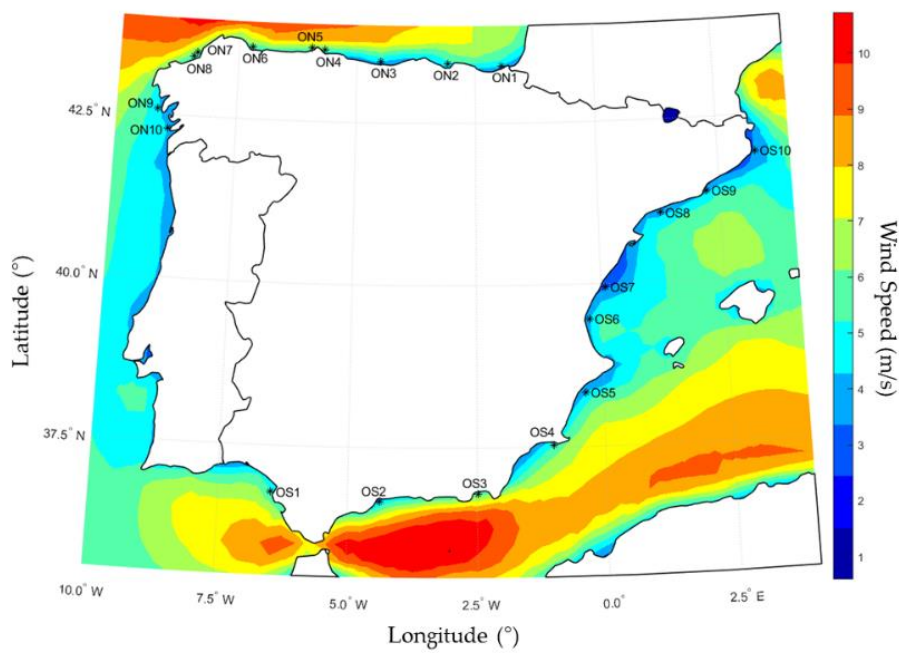


Figure 3. U_{100} wind map for the coastal environment of the Iberian Peninsula, based on a 20-year period of wind data (1999–2018), from ERA5 dataset.

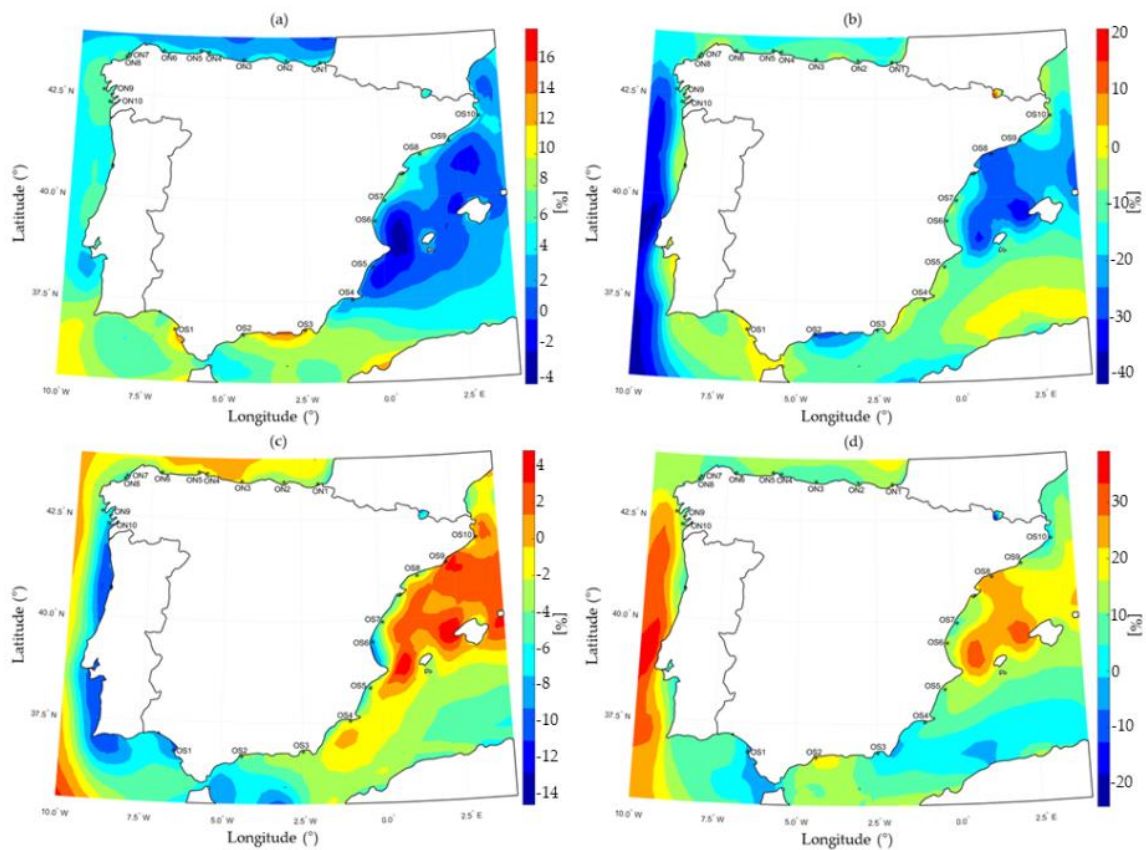


Figure 4. The spatial differences (in %) between the total time data and the main seasons. The results are reported for the U_{100} parameter considering the 20-year period of wind data (1999–2018), from ERA5 dataset, where (a) spring; (b) summer; (c) autumn; (d) winter.

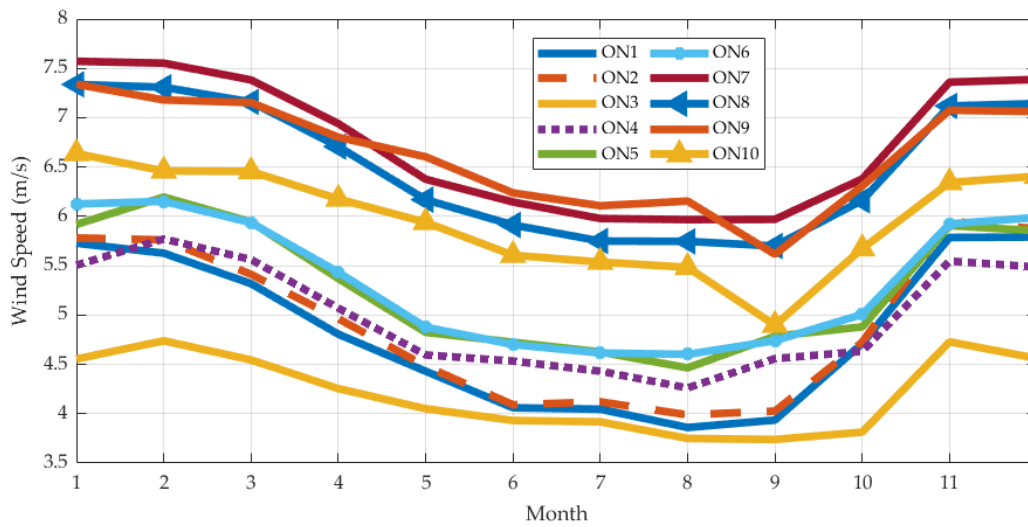


Figure 5. U_{100} monthly values for the points from the North sector.

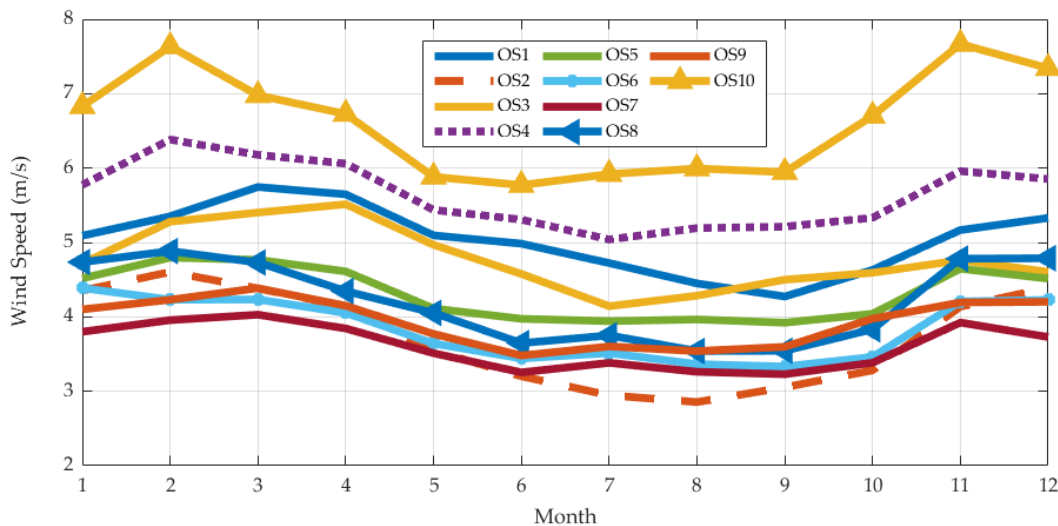


Figure 6. U_{100} monthly values for the points from the South sector.

Looking at the values presented in Tables 3 and 4 and in Figure 3, we can notice some differences. Thus, although the general wind pattern indicated by the map is in line with other similar studies, some differences occur at the land-water interface. The most probable explanation is related to the grid resolution considered ($0.25^\circ \times 0.25^\circ$) and a finer grid will most likely solve this issue. In addition, it is important to mention that on land, a mask is applied over the wind field (covering both land and marine regions), and although the differences are not visible, they are significant in the sense that the onshore wind is considerably lower onshore. This can lead to interferences near the coasts, and the map presented in Figure 3, although providing a general picture of the offshore wind energy resources distribution around the Iberian Peninsula, is not sensitive enough to provide a very correct representation close to the coast.

As mentioned in the previous section, the study approximates the wind speed (U_{100}) to the two parameter Weibull distribution, and Table 6 represents the values of the shape parameter (k) and the scale parameter (c) for all the points considered. With a maximum c value of 7.619 m/s in the point ON7 and a minimum value of 4.059 m/s, in OS7, in these points the wind speed follows the most and least variable Weibull probabilistic distribution, respectively. The parameter k shows values between 2.111 in ON7 and 0.831 in ON1. These imply that the above-mentioned locations present the distributions that show U_{100} wind speed values of greater and lesser magnitude, respectively.

All this information contained in Table 6 is accompanied by the graphic representation of the Weibull probabilistic distribution for the North sector points in Figure 7, this same representation is presented for the South sector locations in Figure 8.

Table 6. Weibull parameters for the U_{100} distribution for each location selected.

| North Sector | ON1 | ON2 | ON3 | ON4 | ON5 | ON6 | ON7 | ON8 | ON9 | ON10 |
|--------------|-------|-------|-------|-------|-------|-------|-------|-------|-------|-------|
| c (m/s) | 5.459 | 5.566 | 4.747 | 5.626 | 5.955 | 6.024 | 7.619 | 7.355 | 7.489 | 6.735 |
| k | 1.831 | 1.938 | 1.819 | 1.837 | 1.821 | 1.959 | 2.111 | 2.084 | 2.021 | 1.941 |
| South Sector | OS1 | OS2 | OS3 | OS4 | OS5 | OS6 | OS7 | OS8 | OS9 | OS10 |
| c (m/s) | 5.692 | 4.211 | 5.368 | 6.363 | 4.867 | 4.321 | 4.059 | 4.742 | 4.438 | 7.431 |
| k | 2.092 | 1.844 | 1.749 | 1.943 | 1.936 | 1.787 | 1.725 | 1.728 | 1.809 | 1.713 |

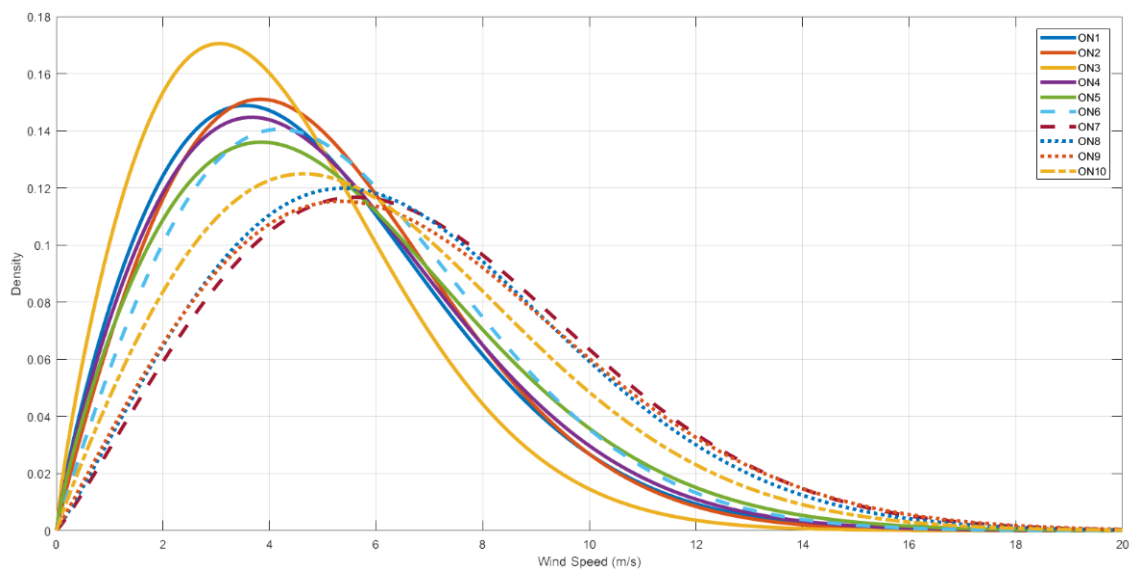


Figure 7. The Weibull distribution corresponding to U_{100} values for the points from the North sector.

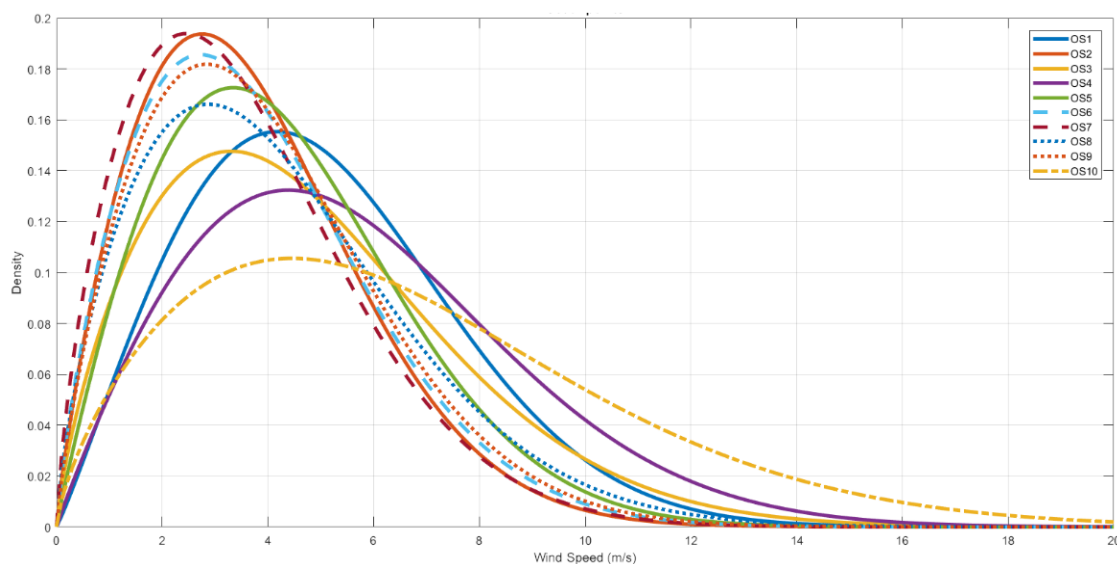


Figure 8. The Weibull distribution corresponding to U_{100} values for the points from the South sector.

Table 7 shows the classification of the wind at the operational height considered (100 m above sea level) from C1 to C7 depending on the wind speed value (U_{100}) as well as its wind power density (P_{wind}). Wind speed accommodates values ranging from the interval 0–5.05 m/s for C1 to 8.04–10.8 m/s for C7.

This corresponds to wind power density values from 0–114.87 W/m² for C1 to 459.50–1148.75 W/m² for C7. These intervals presented in Table 7 are the classification criteria followed in order to obtain Figure 9, which is composed by four maps of the Iberian Peninsula representing the percentage of wind that belongs to classes C1, C3, C5 and C7, respectively.

Table 7. Wind energy scale at elevation of 100 m.

| Wind Power Class | Wind Speed (m/s) | Wind Power Density (W/m ²) |
|------------------|------------------|--|
| C1 (Poor) | 0–5.05 | 0–114.87 |
| C2 (Marginal) | 5.05–5.86 | 114.87–172.31 |
| C3 (Fair) | 5.86–6.43 | 172.31–229.75 |
| C4 (Good) | 6.43–6.89 | 229.75–287.19 |
| C5 (Excellent) | 6.89–7.35 | 287.19–344.62 |
| C6 (Outstanding) | 7.35–8.04 | 344.62–459.50 |
| C7 (Superb) | 8.04–10.80 | 459.50–1148.75 |

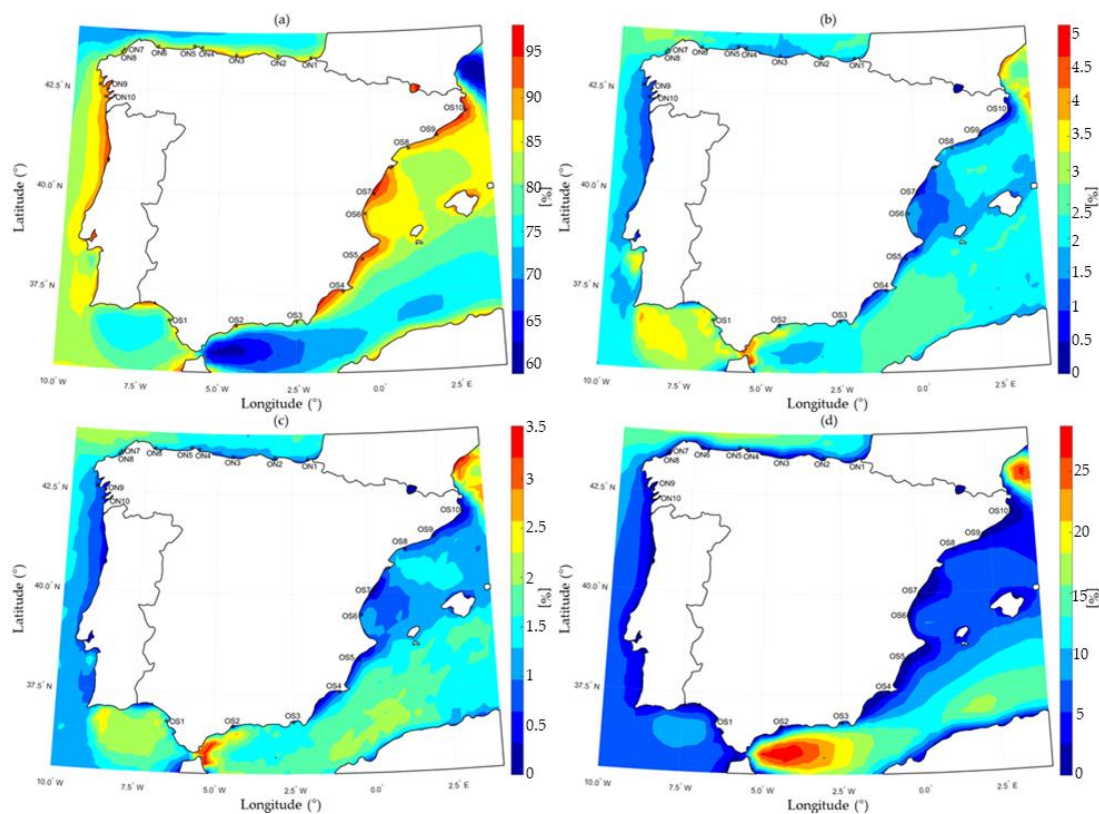


Figure 9. Wind map for wind classes for the coastal environment of the Iberian Peninsula, based on a 20-year period of wind data (1999–2018), from ERA-5 dataset, where (a) C1; (b) C3; (c) C5; (d) C7.

In the previous section, another relevant classification was mentioned, the so-called IEC wind turbine classes. From this perspective, Figure 10 represents graphically over three maps of the Iberian Peninsula, the classification of the wind turbines for IEC Class 1, Class 2, and Classes 3 to 4 respectively. Practically, the entire coastal territory is classified within Classes 3 and 4, however, in the areas corresponding to the points that have consistently been showing the best characteristics. This is the case of the points ON7, ON9 in the North sector or OS4 and OS10 in the South sector, as there are hot-spots there that would be classified as Class 2—some of them even as Class 1.

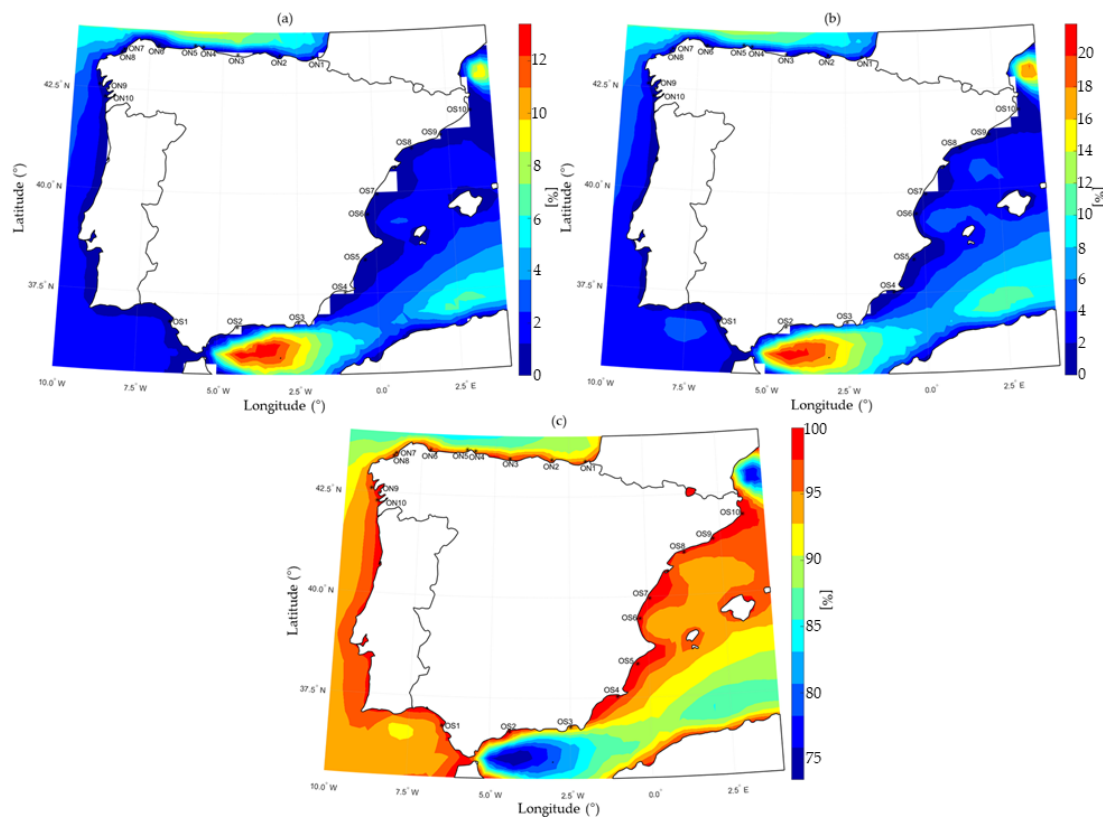


Figure 10. IEC wind turbine class map for the coastal environment of the Iberian Peninsula, based on a 20-year period of wind data (1999–2018), from ERA-5 dataset, where (a) Class 1; (b) Class 2; (c) Classes 3 and 4.

Reviewing the results obtained after studying the performance of the wind turbine technologies considered, Figure 11 represents the *AEP* of each of the four wind turbines in each of the 20 locations along the Spanish coastal environment. Generally, the points located in the North sector have a higher energy production, and this is to be expected due to the fact that all previous results indicate that the Atlantic Coasts resources are generally superior to those of the Mediterranean Coast, where only the OS4 and OS10 present values of similar magnitude to the North sector ones. It is relevant to mention that the energy productions of the V164-8.8 and V164-9.5 turbines are practically equal and much higher than those presented by the Areva M5000-116 or V90-3.0 turbine. This is to be expected as both V164 wind turbine technologies have a considerably higher rated capacity than the remaining two.

The remaining relevant energetic parameter that provides information regarding the performance of each wind turbine technology considered is the capacity factor (C_f). The values of this parameter are illustrated in Figure 12 for each of the wind turbines in the North sector locations. Analogously, Figure 13 represents these values for the locations of the South sector. The highest capacity factor values result in the North sector points, where once again the reference point ON7 corresponds the highest value for the Areva M500-116 wind turbine that manages to provide a better performance. In the South sector, the OS10 location is the one that presents better values.

Finally, in order to conclude this section, it can be highlighted that the results presented provide significant information and represent a good base for the identification of the most relevant locations for the development of offshore wind farms.

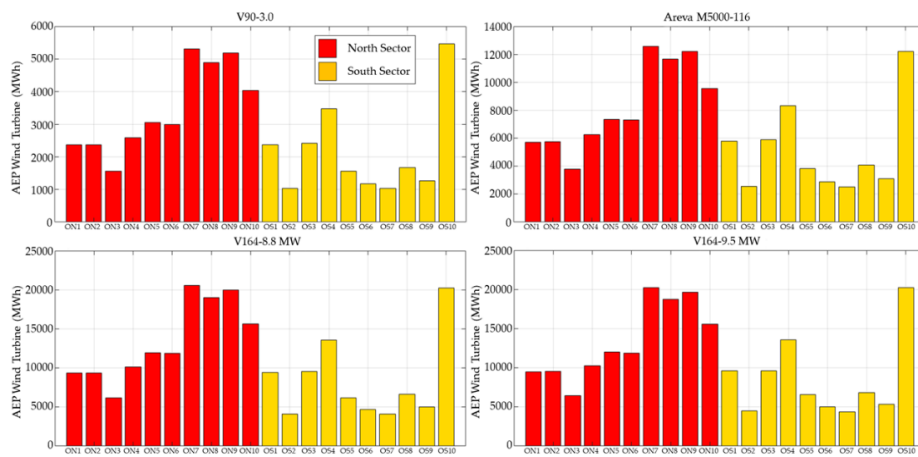


Figure 11. AEP of each wind turbine in the reference points considered.

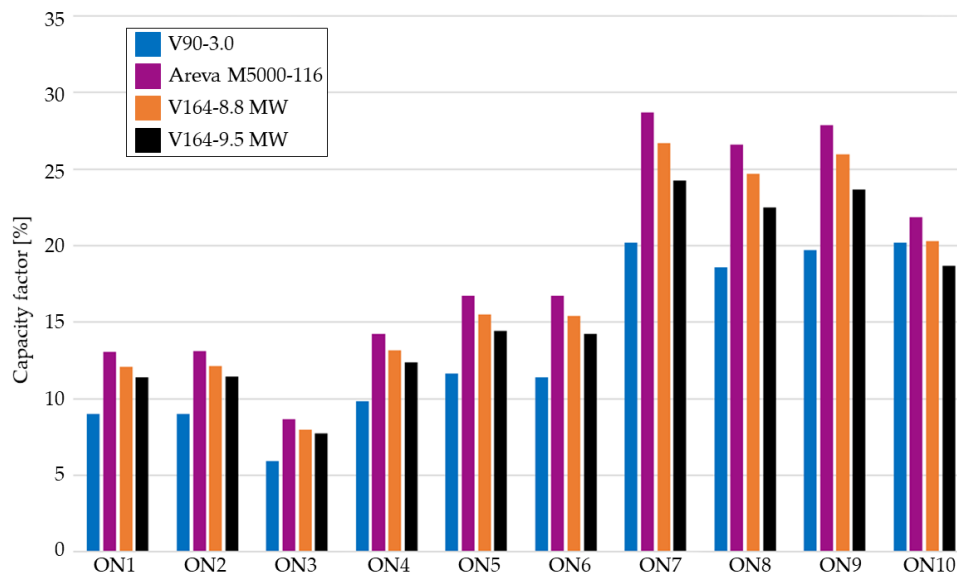


Figure 12. Capacity factor (C_f) of each wind turbine in the points from the North sector.

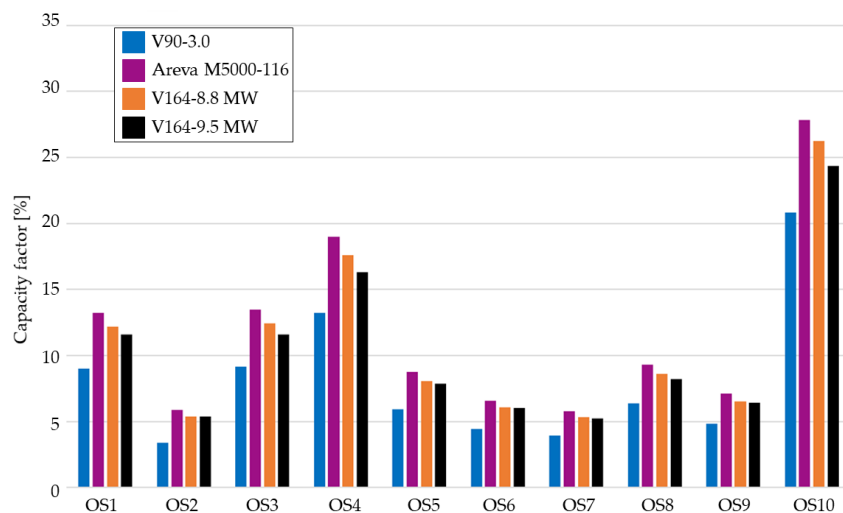


Figure 13. Capacity factor (C_f) of each wind turbine in the points from the South sector.

4. Discussion

In this section, an analysis of the results obtained in the present study will be made together with a comparison with some other significant works. In general, it can be noted that the points located on the North sector present higher average wind speed (U_{100}), with values above 4.21 m/s in all the locations considered along the Atlantic Coast.

In regard to the Southern part, in Sánchez-Lozano et al. [49] the mean wind speed values reported at 10 m height in the Murcia region are between 2.49 and 3.52 m/s. The present study shows a total wind speed value at the operational height (100 m) of 5.64 m/s for the 20-year period considered in the location OS4, which is very close to this region. Taking into consideration the increase in the wind speed values that takes place when translating to a greater height, which is analyzed in Cabello and Orza [50]. In this study, which is focused on the same geographical area, an increase of 30% is estimated when translated from 2 to 10 m height. It is also of special relevance to highlight the enhancement of the average wind speed when going from onshore to offshore, a feature that is characteristic for the entire Iberian nearshore.

It is also relevant to mention the location OS10, which is placed very close to the Franco-Spanish border, as the obtained results show a total wind speed (U_{100}) mean value of 6.61 m/s with a maximum mean value of 7.26 m/s during the months of December to February, corresponding to the winter season. In Pascual et al. [51], the high seasonal variability, due to the wind pattern known as Tramontana, is highlighted. This feature characterizes the Balearic Mediterranean area, corresponding to the points OS4 to OS10. This variability is shown in the results presented in Figures 4 and 6, where it is illustrated how these points have a seasonal mean value increase up to 25% when compared to the total historical (U_{100}) means.

Regarding the two parameters corresponding to the Weibull probabilistic distribution, no unusual values are observed. Thus, the ON1 location presents values of 5.459 m/s and 1.831 for the scale (c) and shape (k) parameters, respectively. In Herrero-Novoa et al. [52], values for these Weibull distribution characteristic parameters are obtained based on field measurements, reported at 2, 10, and 50 m height from the meteorological stations distributed throughout Navarra region (42° N, -1° E). Since the values of the two parameters corresponding to the Weibull distribution are 4.98 m/s and 2.07 for c and k , respectively, when considering a 50 m height. From this perspective, it is relevant to mention that the operational height taken into account in the present study is 100 m above sea level. These values present sufficient concordance with the results obtained in the present study at the location ON1.

As a concise representation of the wind capacities [31,34], Figure 9 represents the classification map of the wind classes for the Iberian Peninsula. With this representation it can once again be highlighted that the North sector shows higher wind classes, reaching values up to 15% for Class 7 in some locations. This is equivalent to a wind power density (P_{wind}) between 459.5 W/m² and 1148.75 W/m². When comparing these percentages with less than 1% presented by the nearby onshore areas [52], it is viable to notice once again that generally offshore areas have better wind resources along all the Spanish continental nearshore, with the Atlantic Coast showing a special predominance as regards the offshore wind resources.

Figure 11 represents the values obtained for the Annual Electricity Production (AEP) parameter for each of the wind turbine technologies considered, the highest values being located in the North sector with reference points ON7 to ON9. OS10 is the only South sector point with comparable production values. According to the data presented in the official Annual Electricity Demand Revision for 2019, published by the national entity Red Eléctrica de España [53,54], the Galician region comprising the points ON7 to ON10, had in 2019 a demand of 18,351 GWh. This means that in order to reach a significant value of 1% of this demand, different offshore wind farm configurations should be developed. The lowest number of turbines needed would be obtained by using the V164-8.8 wind turbine technology, when installed in the ON7 location. The results of the present study show that a turbine individually generates around 20,580 MWh in a year, so by installing nine of these wind turbines, 1.0093% of the annual demand of this autonomous region would be generated. On the other

hand, the installation with the highest number of turbines would take place when using the V90-3.0 wind turbine, which when located in ON8 generates 4890 MWh annually. Therefore, it would be necessary to install 38 of these wind turbines in order to generate 1.0125% of the annual demand. Due to the higher consumption in the region where the OS10 point is located, corresponding to Catalonia with an annual demand of 46,873 GWh, achieving these percentage values would entail much greater economic investments.

However, the *AEP* is not the only relevant parameter to be considered for the wind turbines. It is also of great importance to take into account the capacity factor (C_f). Both Figures 12 and 13 show how the Areva M500-116 wind turbine presents the best C_f for each of the 20 locations considered in the study. If once again we analyze the installation that would need to be developed in order to generate 1% of the *AEP* of the Galicia region, it would take 15 wind turbines generating a total amount of 188,550 MWh annually when located in ON7 (equivalent to 1.0275% of the *AEP* of the Galicia region). With a C_f of 28.5%, higher than the 26% of the aforementioned V164-8.8, the installation of the wind turbine technology with a better C_f could be considered of higher interest.

Referring to other works, such as in Ramírez et al. [55], which presented a similar study for the onshore territory of the Iberian Peninsula, where three different onshore wind farm installations were considered, it can be concluded that the mean value of C_f for the 2016 year is around 24%. This value is consistent with the one mentioned in Migoya et al. [56], where while considering a lower annual operating hours value, C_f for an onshore wind farm located in Madrid is again estimated to be 24%. This, far from being considered an indisputable average value, provides a general image of the values that can be expected to take place for C_f when considering onshore locations in the Iberian Peninsula.

Seeking to highlight the common objective of renewable energies, and in order to quantify the positive ecological impact that the installation of an offshore wind farm would provide to the Spanish nearshore environment, the CO₂ equivalent emissions avoidance parameter was also considered to be of special relevance in this study. From this perspective, Figure 14 shows the results obtained for each of the wind turbines considered when located in each of the 20 study locations, as calculated using Equation (7). The results show how the emission of 15.02 t/MWh would be avoided if turbines V164-8.8 are located in ON7.

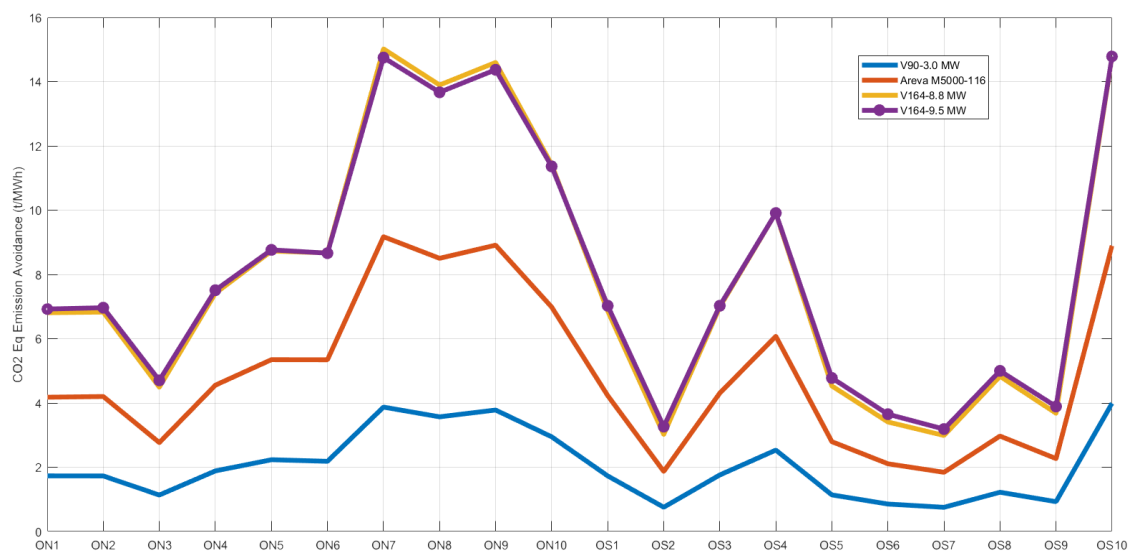


Figure 14. CO₂ equivalent emission avoidance (tons/MWh) of each wind turbine in the reference points considered.

However, the data presented in the CO₂ electricity generation associated emissions, published in May 2020 by the national entity Red Eléctrica de España [53,57], consider this avoidance to be equivalent to 100% of the *AEP* values multiplied by 1×10^{-3} . Meanwhile, when computing the x and y

parameters of the Equation (7), it results on only considering an emission avoidance equivalent to the AEP value multiplied by approximately 0.73×10^{-3} . So, if the methodology applied by the Spanish entity is considered, the values for this parameter would be somewhat higher.

In addition to this, it is relevant to mention that the Iberian Peninsula is an important area for the wind and wave resources and as a consequence during the recent years several studies discussed the benefits of using both resources in combined wind-wave projects [57–61]. Although the wave energy is more significant than the wind energy, the wave industry is still in an infancy stage so that the know-how accumulated by the wind sector could be useful. Among the benefits outlined by the authors, these benefits can be mentioned as more relevant: reducing the intermittency of the power production, improving the CAPEX and OPEX values, and providing coastal protection.

5. Conclusions

In this study, an assessment of the wind resources along the Spanish continental nearshore has been made, taking into account the wind characteristics evaluated for 20 locations along this coastal environment. In addition, the characteristic power curves of some wind turbines were considered, all of them being already present at this moment in operational projects.

Furthermore, by taking some other aspects into consideration, such as maritime traffic or the presence of natural exclusion areas, a selection has been made within the points that present better wind resources.

From this perspective, it was concluded that, the points located in the North sector generally have the best characteristics when evaluating the possible development of an offshore wind farm, although encouraging particularities were also found in some points from the Southern area. This is the case of OS4, corresponding to the Strait of Gibraltar, and the point OS10, corresponding to the French border in the Balearic Mediterranean zone. However, it can be noticed that these two locations are the only points of real relevance in the South sector.

Due to factors, such as maritime traffic, high population density or the presence of protected natural areas, the point OS4 was discarded, considering that the resources of this location are not high enough to overcome the impediments mentioned that could lead to incurring on higher costs.

Regarding the OS10 location, the aforementioned characteristic variability of the wind resources in that region indicates that other locations with more stable wind resources throughout the year should be more viable for an offshore wind farm project development. This added to the very high population density in this region, which would lead to discard the OS10 location as well.

Focusing now on the North sector, the locations with the best offshore wind resources are those from the region of Galicia, with the reference points ON7, ON8 and ON9 being the most favorable. However, points such as ON10, ON3, ON4, or ON5 are not discarded, since various aforementioned studies conclude that these locations present high wave energy resources, so a hybrid approach could be of special relevance in some areas. Therefore, in general it is relevant to mention the fact that the Northern side of the Iberian nearshore has also a very good potential in terms of wave energy resources. From this perspective, this coastal environment represents an optimal target for the development of hybrid wind-waves marine energy farms. Besides the fact that such marine energy farms can become a viable source of clean energy, another important aspect related to the marine renewable energy is that its extraction can influence in a significant way the coastal dynamics, and thus can have a beneficial influence in providing coastal protection.

Author Contributions: The conceptualization belongs to E.R. F.O. established the methodology and perform the validation. A.R. performed the formal analysis, the investigation, data curation and prepared the original draft of the manuscript. E.R. performed the review and editing and supervision while F.O. The visualization. E.R. was in charge also with the project administration and funding acquisition. All authors have read and agreed to the published version of the manuscript. analyzed the data designing the figures.

Funding: This work was supported by the project “Excellence, performance and competitiveness in the Research, Development and Innovation activities at “Dunarea de Jos” University of Galati”, acronym “EXPERT”, financed by the Romanian Ministry of Research and Innovation in the framework of Programme 1—Development of the national research and development system, Sub-programme 1.2—Institutional Performance —Projects for financing excellence in Research, Development and Innovation, Contract no. 14PFE/17.10.2018.

Acknowledgments: The ERA5 wind data used in this study have been obtained from the ECMWF data server.

Conflicts of Interest: The authors declare no conflict of interest.

References

- al Irsyad, M.I.; Halog, A.; Nepal, R. Renewable Energy Projections for Climate Change Mitigation: An Analysis of Uncertainty and Errors. *Renew. Energy* **2019**, *130*, 536–546. [CrossRef]
- Bhattacharya, M.; Paramati, S.R.; Ozturk, I.; Bhattacharya, S. The Effect of Renewable Energy Consumption on Economic Growth: Evidence from Top 38 Countries. *Appl. Energy* **2016**, *162*, 733–741. [CrossRef]
- Cho, S.; Heo, E.; Kim, J. Causal Relationship between Renewable Energy Consumption and Economic Growth: Comparison between Developed and Less-Developed Countries. *Geosystem Eng.* **2015**, *18*, 284–291. [CrossRef]
- Bhattacharyya, S.C.; Timilsina, G.R. A Review of Energy System Models. *Int. J. Energy Sect. Manag.* **2010**, *4*, 494–518. [CrossRef]
- Saad, W.; Taleb, A. The Causal Relationship between Renewable Energy Consumption and Economic Growth: Evidence from Europe. *Clean Technol. Environ. Policy* **2018**, *20*, 127–136. [CrossRef]
- Wu, X.; Hu, W.; Huang, Q.; Chen, C.; Chen, Z.; Blaabjerg, F. Optimized Placement of Onshore Wind Farms Considering Topography. *Energies* **2019**, *12*, 2944. [CrossRef]
- Poulsen, T.; Hasager, C. The (R)evolution of China: Offshore Wind Diffusion. *Energies* **2017**, *10*, 2153. [CrossRef]
- Onea, F.; Rusu, L. Evaluation of Some State-Of-The-Art Wind Technologies in the Nearshore of the Black Sea. *Energies* **2018**, *11*, 2452. [CrossRef]
- Rusu, E.; Venugopal, V. Special Issue “Offshore Renewable Energy: Ocean Waves, Tides and Offshore Wind”. *Energies* **2019**, *12*, 182. [CrossRef]
- Willis, D.J.; Niezrecki, C.; Kuchma, D.; Hines, E.; Arwade, S.R.; Barthelmie, R.J.; DiPaola, M.; Drane, P.J.; Hansen, C.J.; Inalpolat, M.; et al. Wind Energy Research: State-Of-The-Art and Future Research Directions. *Renew. Energy* **2018**, *125*, 133–154. [CrossRef]
- Castro-Santos, L.; Martins, E.; Guedes Soares, C. Methodology to Calculate the Costs of a Floating Offshore Renewable Energy Farm. *Energies* **2016**, *9*, 324. [CrossRef]
- Montoya, F.G.; Aguilera, M.J.; Manzano-Agugliaro, F. Renewable Energy Production in Spain: A Review. *Renew. Sustain. Energy Rev.* **2014**, *33*, 509–531. [CrossRef]
- Child, M.; Breyer, C. The Role of Energy Storage Solutions in a 100% Renewable Finnish Energy System. *Energy Procedia* **2016**, *99*, 25–34. [CrossRef]
- Perez, Y.; Ramos-Real, F.J. The Public Promotion of Wind Energy in Spain from the Transaction Costs Perspective 1986–2007. *Renew. Sustain. Energy Rev.* **2009**, *13*, 1058–1066. [CrossRef]
- Colmenar-Santos, A.; Perera-Perez, J.; Borge-Diez, D.; dePalacio-Rodríguez, C. Offshore Wind Energy: A Review of the Current Status, Challenges and Future Development in Spain. *Renew. Sustain. Energy Rev.* **2016**, *64*, 1–18. [CrossRef]
- Ishie, J.; Wang, K.; Ong, M. Structural Dynamic Analysis of Semi-Submersible Floating Vertical Axis Wind Turbines. *Energies* **2016**, *9*, 1047. [CrossRef]
- Yang, W.; Tian, W.; Hvalbye, O.; Peng, Z.; Wei, K.; Tian, X. Experimental Research for Stabilizing Offshore Floating Wind Turbines. *Energies* **2019**, *12*, 1947. [CrossRef]
- Radowitz, B.; Snieckus, D. Spain Grants Equinor Ok for World’s Biggest Floating Wind Farm | Recharge. Available online: <https://www.rechargenews.com/wind/spain-grants-equinor-ok-for-worlds-biggest-floating-wind-farm/2-1-615375> (accessed on 25 May 2020).
- Russell, T. Equinor Eyes Canary Island Project | 4C Offshore News. Available online: <https://www.4coffshore.com/news/equinor-eyes-canary-island-project-nid13740.html> (accessed on 4 May 2020).
- Página Inicio | puertos.es. Available online: <http://www.puertos.es/es-es> (accessed on 10 June 2020).

21. Prediccion de oleaje, nivel del mar; Boyas y mareografos | puertos.es. Available online: <http://www.puertos.es/es-es/oceanografia/Paginas/portus.aspx> (accessed on 10 June 2020).
22. Bathymetric Data Viewer. Available online: <https://maps.ngdc.noaa.gov/viewers/bathymetry/> (accessed on 19 May 2020).
23. ERA5 | ECMWF. Available online: <https://www.ecmwf.int/en/forecasts/datasets/reanalysis-datasets/era5> (accessed on 10 June 2020).
24. Dee, D.P.; Uppala, S.M.; Simmons, A.J.; Berrisford, P.; Poli, P.; Kobayashi, S.; Andrae, U.; Balmaseda, M.A.; Balsamo, G.; Bauer, P.; et al. The ERA-Interim Reanalysis: Configuration and Performance of the Data Assimilation System. *Q. J. R. Meteorol. Soc.* **2011**, *137*, 553–597. [[CrossRef](#)]
25. Hersbach, H.; Bell, B.; Berrisford, P.; Hirahara, S.; Horányi, A.; Muñoz-Sabater, J.; Nicolas, J.; Peubey, C.; Radu, R.; Schepers, D.; et al. The ERA5 Global Reanalysis. *Q. J. R. Meteorol. Soc.* **2020**, 1–51. [[CrossRef](#)]
26. Download MATLAB, Simulink, Stateflow and Other MathWorks Products. Available online: <https://www.mathworks.com/downloads/> (accessed on 10 June 2020).
27. Bauer, L. AREVA M5000-116-5,00 MW—Wind Turbine. Available online: <https://en.wind-turbine-models.com/turbines/23-areva-m5000-116> (accessed on 19 May 2020).
28. Bauer, L. MHI Vestas Offshore V164-8.8 MW-8,80 MW—Wind Turbine. Available online: <https://en.wind-turbine-models.com/turbines/1819-mhi-vestas-offshore-v164-8.8-mw> (accessed on 19 May 2020).
29. MHI Vestas Offshore V164/9500—Manufacturers and Turbines—Online Access—The Wind Power. Available online: https://www.thewindpower.net/turbine_en_1476_mhi-vestas-offshore_v164-9500.php (accessed on 19 May 2020).
30. Vestas V90-3.0-3,00 MW—Wind Turbine. Available online: <https://en.wind-turbine-models.com/turbines/603-vestas-v90-3.0> (accessed on 19 May 2020).
31. Diaconita, A.; Onea, F.; Rusu, E. An Evaluation of the Wind Energy in the North Sea Coast. *Mech. Test. Diagn.* **2019**, *9*, 17–22. [[CrossRef](#)]
32. Ziegler, L.; Gonzalez, E.; Rubert, T.; Smolka, U.; Melero, J.J. Lifetime Extension of Onshore Wind Turbines: A Review Covering Germany, Spain, Denmark, and the UK. *Renew. Sustain. Energy Rev.* **2018**, *82*, 1261–1271. [[CrossRef](#)]
33. Kubik, M.L.; Coker, P.J.; Hunt, C. Using Meteorological Wind Data to Estimate Turbine Generation Output: A Sensitivity Analysis. In Proceedings of the Conference of World Renewable Energy Congress, Linköping, Sweden, 8–13 May 2011; pp. 4074–4081.
34. Onea, F.; Deleanu, L.; Rusu, L.; Georgescu, C. Evaluation of the Wind Energy Potential along the Mediterranean Sea Coasts. *Energy Explor. Exploit.* **2016**, *34*, 766–792. [[CrossRef](#)]
35. *Offshore Renewable Energy: Ocean Waves, Tides and Offshore Wind*; MDPI: Basel, Switzerland, 2019, ISBN 978-3-03897-593-9.
36. Archer, C.L.; Jacobson, M.Z. Spatial and Temporal Distributions of U.S. Winds and Wind Power at 80 m Derived from Measurements: Feasibility of U.S. Wind Power. *J. Geophys. Res. Atmos.* **2003**, *108*. [[CrossRef](#)]
37. Spinato, F.; Tavner, P.J.; van Bussel, G.J.W.; Koutoulakos, E. Reliability of Wind Turbine Subassemblies. *IET Renew. Power Gener.* **2009**, *3*, 387. [[CrossRef](#)]
38. Honrubia-Escribano, A.; Jiménez-Buendía, F.; Gómez-Lázaro, E.; Fortmann, J. Validation of Generic Models for Variable Speed Operation Wind Turbines Following the Recent Guidelines Issued by IEC 61400-27. *Energies* **2016**, *9*, 1048. [[CrossRef](#)]
39. Weisser, D. A Wind Energy Analysis of Grenada: An Estimation Using the ‘Weibull’ Density Function. *Renew. Energy* **2003**, *28*, 1803–1812. [[CrossRef](#)]
40. Shu, Z.R.; Li, Q.S.; Chan, P.W. Statistical Analysis of Wind Characteristics and Wind Energy Potential in Hong Kong. *Energy Convers. Manag.* **2015**, *101*, 644–657. [[CrossRef](#)]
41. Al-Nassar, W.; Alhajraf, S.; Al-Enizi, A.; Al-Awadhi, L. Potential Wind Power Generation in the State of Kuwait. *Renew. Energy* **2005**, *30*, 2149–2161. [[CrossRef](#)]
42. Chang, T.P. Estimation of Wind Energy Potential Using Different Probability Density Functions. *Appl. Energy* **2011**, *88*, 1848–1856. [[CrossRef](#)]
43. Rusu, E.; Onea, F. An Assessment of the Wind and Wave Power Potential in the Island Environment. *Energy* **2019**, *175*, 830–846. [[CrossRef](#)]
44. Salvação, N.; Guedes Soares, C. Wind Resource Assessment Offshore the Atlantic Iberian Coast with the WRF Model. *Energy* **2018**, *145*, 276–287. [[CrossRef](#)]

45. Ciulla, G.; D'Amico, A.; Di Dio, V.; Lo Brano, V. Modelling and Analysis of Real-World Wind Turbine Power Curves: Assessing Deviations from Nominal Curve by Neural Networks. *Renew. Energy* **2019**, *140*, 477–492. [[CrossRef](#)]
46. Onea, F.; Rusu, E. Efficiency Assessments for some State of the Art Wind Turbines in the Coastal Environments of the Black and the Caspian Seas. *Energy Explor. Exploit.* **2016**, *34*, 217–234. [[CrossRef](#)]
47. Arun Kumar, S.V.V.; Nagababu, G.; Sharma, R.; Kumar, R. Synergetic Use of Multiple Scatterometers for Offshore Wind Energy Potential Assessment. *Ocean Eng.* **2020**, *196*, 106745. [[CrossRef](#)]
48. Greenhouse Gases Equivalencies Calculator - Calculations and References | Energy and the Environment | US EPA. Available online: <https://www.epa.gov/energy/greenhouse-gases-equivalencies-calculator-calculations-and-references> (accessed on 15 July 2020).
49. Sánchez-Lozano, J.M.; García-Cascales, M.S.; Lamata, M.T. Identification and Selection of Potential Sites for Onshore Wind Farms Development in Region of Murcia, Spain. *Energy* **2014**, *73*, 311–324. [[CrossRef](#)]
50. Cabello, M.; Orza, J.A.G. Wind speed analysis in the province of Alicante, Spain. Potential for Small-Scale Wind Turbines. *Renew. Sustain. Energy Rev.* **2010**, *14*, 3185–3191. [[CrossRef](#)]
51. Pascual, A.; Martín, M.L.; Valero, F.; Luna, M.Y.; Morata, A. Wintertime Connections between Extreme Wind Patterns in Spain and Large-Scale Geopotential Height Field. *Atmos. Res.* **2013**, *122*, 213–228. [[CrossRef](#)]
52. Herrero-Novoa, C.; Pérez, I.A.; Sánchez, M.L.; García, M.Á.; Pardo, N.; Fernández-Duque, B. Wind Speed Description and Power Density in Northern Spain. *Energy* **2017**, *138*, 967–976. [[CrossRef](#)]
53. Inicio | Red Eléctrica de España. Available online: <https://www.ree.es/es> (accessed on 18 June 2020).
54. Boletín Mensual. Noviembre 2019 | Red Eléctrica de España. Available online: <https://www.ree.es/es/datos/publicaciones/boletines-mensuales/boletin-mensual-noviembre-2019> (accessed on 4 May 2020).
55. Ramírez, F.J.; Honrubia-Escribano, A.; Gómez-Lázaro, E.; Pham, D.T. The Role of Wind Energy Production in Addressing the European Renewable Energy Targets: The Case of Spain. *J. Clean. Prod.* **2018**, *196*, 1198–1212. [[CrossRef](#)]
56. Migoya, E.; Crespo, A.; Jiménez, Á.; García, J.; Manuel, F. Wind Energy Resource Assessment in Madrid Region. *Renew. Energy* **2007**, *32*, 1467–1483. [[CrossRef](#)]
57. Registro de huella de carbono, compensación y proyectos de absorción de dióxido de carbono. Available online: https://www.miteco.gob.es/es/cambio-climatico/temas/mitigacion-politicas-y-medidas/factores_emision_tcm30-479095.pdf (accessed on 15 June 2020).
58. Bento, A.R.; Rusu, E.; Martinho, P.; Guedes Soares, C. Assessment of the Changes Induced by a Wave Energy Farm in the Nearshore Wave Conditions. *Comput. Geosci.* **2014**, *71*, 50–61. [[CrossRef](#)]
59. Rusu, E.; Onea, F. Estimation of the Wave Energy Conversion Efficiency in the Atlantic Ocean Close to the European Islands. *Renew. Energy* **2016**, *85*, 687–703. [[CrossRef](#)]
60. Astariz, S.; Iglesias, G. Output Power Smoothing and Reduced Downtime Period by Combined Wind and Wave Energy Farms. *Energy* **2016**, *97*, 69–81. [[CrossRef](#)]
61. Gaughan, E.; Fitzgerald, B. An Assessment of the Potential for Co-Located Offshore Wind and Wave Farms in Ireland. *Energy* **2020**, *200*, 117526. [[CrossRef](#)]

